Bulk and Surface Structures of Palladium-Modified Copper−Zinc Oxides *ex* Hydroxycarbonate Precursors

I. Melián-Cabrera, M. López Granados, and J. L. G. Fierro*

Instituto de Catálisis y Petroleoquímica, CSIC, Cantoblanco, 28049 Madrid, Spain

Received November 19, 2001. Revised Manuscript Received February 1, 2002

(Pd)−Cu−Zn *ex* hydroxycarbonate precursors were prepared and characterized by several bulk and surface techniques. A palladium-free Cu−Zn precursor (CZ) was prepared by coprecipitation. Two Pd−Cu−Zn samples were prepared by coprecipitation (PCZ-CP) and sequential precipitation (PCZ-SP). It is shown that the surface and bulk structures of Pd-modified precursors depend on the palladium incorporation methodology. This effect does not appear to be influenced by palladium incorporation itself but results from the conditions used in the preparation of the materials, more specifically the sodium concentration from the precipitating agent Na_2CO_3. A higher Na_2CO_3 concentration was needed in the preparation of PCZ-CP than for the other precursors. The higher Na concentration in the synthesis medium affects the growth of the sodium−zinc carbonate precursor and gives rise to the formation of independent Cu and Zn phases in the final precursor. The interaction between CuO and ZnO in the calcined state is then inhibited, resulting in an increase in the particle size of both oxidic phases. The lower Na concentration used during the synthesis of the materials CZ and PCZ-SP favors the development of an aurichalcite phase, a structure in which the Cu and Zn are atomically dispersed in a hydroxycarbonate matrix. This leads to finely dispersed copper and zinc mixed oxides with smaller particle sizes than those derived from independent Cu and Zn precursor phases, as in the case of PCZ-CP.

1. Introduction

Copper-containing catalytic materials are widely used for hydrogenation reactions and, in particular, for methanol synthesis through CO/CO_2 hydrogenation. Because of the rather low Hutting's temperature of copper (450 K, calculated as one-third of the melting temperature), i.e., the temperature at which the mobility of the copper atoms on the catalyst surface becomes important, a significant loss of Cu dispersion occurs during catalyst activation and reaction. This problem can be overcome by intimate mixing of the copper phase with at least one other oxidic component. The copper phase is then stabilized, and the interaction with the host oxide is also enhanced. One possibility of obtaining a good intimate mixing of the catalyst components is the formation of a precursor by means of coprecipitation from which the oxidic phases are obtained by thermal decomposition.[1] The preparation of the conventional $CuO-ZnO(-Al_2O_3)$-based systems involves a coprecipitation method in which an aqueous solution of copper, zinc, and aluminum nitrates is mixed with a sodium carbonate solution.[2−4] This procedure leads to the formation of several mixed metal hydroxycarbonates such as aurichalcite, $(Cu,Zn)_5(CO_3)_2(OH)_6$, zincian−malachite (or rosasite), $(Cu,Zn)_2(OH)_2CO_3$, and a Cu−Zn hydrotalcite-like phase $(Cu,Zn)_6Al_2(OH)_{16}CO_3{\cdot}4H_2O$. The kind of precursor formed depends on the preparation conditions (pH and temperature) and the relative metallic composition. If suitable synthesis conditions are not selected, the formation of pure hydroxycarbonates such as malachite $Cu_2(OH)_2CO_3$ and hydrozincite $Zn_5(CO_3)_2(OH)_6$ is favored, resulting in catalysts with a lower copper dispersion.

Although the conventional $CuO-ZnO-Al_2O_3$ mixed oxide catalysts, which are obtained from this classical hydroxycarbonate route, have achieved excellent results in the industrial synthesis of methanol, there have been many claims that the catalyst performance can be improved by increasing the dispersion of the copper phase as well as by adding a promoter other than a mere copper dispersion enhancing agent. Examples of methods that try to increase the copper dispersion include ultrasonic treatment during the hydroxycarbonate formation,[5] the new intrinsic uniform gelation method,[6] the oxalate gel-coprecipitation method,[7] and mechanical mixing of copper and zinc oxide powders.[8,9] Examples of modifiers that can be added to Cu−Zn are chromium,[10] zirconium,[11−13] vanadium,[13] cerium,[14] tita-

* To whom correspondence should be addressed. E-mail: jlgfierro@icp.csic.es. Tel.: +34-91-585-4769. Fax: +34-91-585-4760.

(1) Courty, P.; Marcilly, C. *Stud. Surf. Sci. Catal.* **1983**, *16*, 485.
(2) Klier, K. *Adv. Catal.* **1982**, *31*, 243.
(3) Chinchen, G. C.; Denny, P. J.; Jennings, J. R.; Spencer, M. S.; Waugh, K. C. *Appl. Catal.* **1988**, *36*, 1.
(4) Bart, J. C. J.; Sneeden, R. P. A. *Catal. Today* **1987**, *2*, 1.
(5) Li, J.-L.; Inui, T. *Appl. Catal. A* **1996**, *139*, 87.
(6) Inui, T.; Takeguchi, T. *Catal. Today* **1991**, *10*, 95.
(7) Jingfa, D.; Qi, S.; Yulong, Z.; Songying, C.; Dong, W. *Appl. Catal. A* **1996**, *139*, 75.
(8) Huang, L.; Kramer, G. J.; Wieldraaijer, W.; Brands, D. S.; Poels, E. K.; Castricum, H. L.; Bakker, H. *Catal. Lett.* **1997**, *48*, 55.
(9) Castricum, H. L.; Bakker, H.; Poels, E. K. *Mater. Sci. Eng. A* **2001**, *304*, 418.
(10) Tagawa, T.; Pleizier, G.; Amenomiya, Y. *Appl. Catal.* **1985**, *18*, 285.
(11) Amenomiya, Y. *Appl. Catal.* **1987**, *30*, 57.

10.1021/cm011281s CCC: $22.00
Published on Web 03/27/2002

nium,[15,16] and gallium.[17,18] An attractive possibility is the incorporation of group VIII noble metals within the catalytic system. The noble metals are excellent candidates to activate hydrogen, which then spreads over the neighboring phases through a hydrogen spillover mechanism. This leads to the surface of the catalyst being in a more reduced state, a situation that may further facilitate surface hydrogenation reactions.

Methanol synthesis from a CO_2/H_2 feed has already been improved by either physically mixing a CuO/ZnO catalyst with a Pd catalyst[19,20] or with a Pd-impregnated $CuO-ZnO-Al_2O_3$ catalyst instead of using physical mixtures.[21,22] The enhancement of the catalytic activity for these Pd-modified materials has been attributed to hydrogen spillover from metallic Pd to metallic Cu, which in turn is involved in the elementary steps of CO_2 hydrogenation. Despite the research carried out on the Pd-modified systems, there still exists a lack of agreement on the optimum preparation method for Pd-containing catalysts supported on different oxides. The discrepancies found may be partially due to the fact that the preparation methods are not fully reproducible and may give rise to a nonhomogeneous distribution of the palladium particles on the surface.[23] For the preparation of supported noble metal catalysts, the wet impregnation method followed by drying may be used to apply high loadings of noble metal when the interaction between the active precursor in solution and the support is weak, as is the case for Pd in Cu−Zn(−Al) systems. The maximum loading is limited by the solubility of the precursor in the pore-filling solution. Bearing in mind the fact that Pd(II) is a very acidic cation, which hydrolyzes easily (reactions 1−3) to a hydroxide at pH > 0.75,[24] low dispersion of the metal could be expected.

$$Pd^{2+} + 2H_2O \rightleftarrows Pd(OH)^+ + H_3O^+ \quad (1)$$

$$Pd(OH)^+ + 2H_2O \rightleftarrows Pd(OH)_2(aq) + H_3O^+ \quad (2)$$

$$Pd(OH)_2(aq) \rightleftarrows Pd(OH)_2(s) \quad (3)$$

Accordingly, impregnation of a calcined CuO−ZnO sample does not appear to be an appropriate method to incorporate palladium. It has recently been reported[25,26] that precipitation may be a suitable procedure to add noble metals to conventional heterogeneous systems. This process allows homogeneous distribution of the precious metal inside the precursor matrix, which by further calcination can give rise to well-dispersed metal particles.

In this paper we report the results of our study on the synthesis and characterization of Pd-modified Cu−Zn methanol synthesis hydroxycarbonate precursors prepared by the precipitation route. An understanding of the bulk and surface structures of the precursors was attained by several physical-chemistry techniques. The information gained allows us to propose and discuss a mechanism for the formation of the precursors. The effect of the specific precursor structure on the dispersion of the final oxidic phases was also investigated, and this relationship is of relevance to the final catalytic properties for the methanol synthesis reaction.

2. Experimental Section

2.1. Synthesis of Precursors. A copper−zinc sample (CZ) with a nominal composition of Cu/Zn = 30/70 (atomic ratio) was prepared by coprecipitation of the corresponding metal nitrates with sodium carbonate at constant pH (ca. 7.0) and constant temperature (323 K).[27] The precursor was prepared by simultaneously adding an aqueous solution of copper and zinc nitrates (total metal concentration = 0.3 M) and an aqueous solution of sodium carbonate (0.5 M) into a beaker containing a small amount of deionized water (18 MΩ/cm, as supplied by a Millipore deionizer). The suspension was continuously stirred and kept at the desired pH by adjusting the relative flow rate of the two solutions. The final suspension was aged under stirring (323 K for 4 h) and cooled to room temperature overnight. The precipitate was filtered off, repeatedly washed with sufficient deionized water to remove residual sodium, and dried overnight at 393 K (precursor).

A series of palladium−copper−zinc (PCZ) samples, with a nominal composition of Pd/Cu/Zn = 1.5/28.5/70 (atomic ratio), were prepared by two methods: (i) coprecipitation (PCZ-CP) of all the cations in one step and (ii) sequential precipitation (PCZ-SP). The two routes are depicted in Scheme 1. In the first case (CP), the procedure was similar to the preparation of the CZ precursor except for the starting solutions. The metal nitrates were dissolved in a 15% HNO_3 solution in order to avoid palladium hydrolysis. The precipitating sodium carbonate solution must be more concentrated (2.0 M) to allow pH control during precipitation. In sequential precipitation (SP), palladium was first hydrolyzed (reactions 1−3) in the vessel containing the cations. The $Pd(OH)_2$ suspension containing Cu^{2+} and Zn^{2+} cations and a solution of sodium carbonate (0.5 M) were simultaneously added to the reaction beaker to give rise to Cu−Zn coprecipitation, as previously was explained for the CZ sample. In both cases, the suspensions were continuously stirred and kept at the desired pH (ca. 7) by adjusting the relative flow rate of the two solutions. The Pd-containing precipitates were also aged (323 K for 4 h) under stirring, washed with deionized water to remove residual sodium, and dried overnight at 393 K.

2.2. Characterization Techniques. Powder X-ray diffraction (XRD) patterns of precursors and calcined samples were recorded on a computerized Seifert 3000XRD diffractometer using Cu Kα radiation, a PW 2200 goniometer (Bragg−Brentano $\theta/2\theta$ geometry), a bent graphite monochromator, and an automatic slit. All of the samples were scanned at $10° < 2\theta < 75°$ in the step mode (0.02°, 2 s).

Thermogravimetric analysis (TGA) curves were recorded with a Perkin-Elmer TGS-2 analyzer in conjunction with a Data Station 3700. The sample holder was loaded with 5−10 mg of specimen, and the decomposition of the precursor was

(12) Koeppel, R. A.; Baiker, A.; Schild, C.; Wokaun, W. *Stud. Surf. Sci. Catal.* **1991**, *63*, 59.
(13) Kanoun, N.; Astier, M. P.; Pajonk, G. M. *Catal. Lett.* **1992**, *15*, 231.
(14) Walker, A. P.; Lambert, R. M.; Nix, R. M.; Jennings, J. R. *J. Catal.* **1992**, *138*, 694.
(15) Barrault, J.; Rassoul, Z.; Bettahar, M. M. *Stud. Surf. Sci. Catal.* **1991**, *61*, 367.
(16) Arakawa, H.; Sayama, K.; Okabe, K.; Murakami, A. *Stud. Surf. Sci. Catal.* **1993**, *77*, 389.
(17) Fujitani, T.; Saito, M.; Kanai, Y.; Kakumoto, T.; Watanabe, T.; Nakamura, J.; Uchijima, T. *Catal. Lett.* **1994**, *25*, 271.
(18) Toyir, J.; de la Piscina, P. R.; Fierro, J. L. G.; Homs, N. *Appl. Catal. B* **2001**, *29*, 207.
(19) Inui, T.; Takeguchi, T. *Catal. Today* **1991**, *10*, 95.
(20) Fujimoto, K.; Yu, Y. *Stud. Surf. Sci. Catal.* **1993**, *77*, 393.
(21) Sahibzada, M.; Chadwick, D.; Metcalfe, I. S. *Catal. Today* **1996**, *29*, 367.
(22) Melián-Cabrera, I.; López Granados, M.; Terreros, P.; Fierro, J. L. G. *Catal. Today* **1998**, *45*, 251.
(23) Geus, J. W.; van Veen, J. A. R. *Stud. Surf. Sci. Catal.* **1999**, *123*, 459.
(24) Baes, C. F.; Mesmer, R. E. *Hydrolysis of Cations*; Wiley: New York, 1976.
(25) Cavani, F.; Trifirò, F.; Vaccari, A. *Catal. Today* **1991**, *11*, 173.
(26) Vaccari, A. *Appl. Clay Sci.* **1999**, *14*, 161.
(27) Li, J. L.; Inui, T. *Appl. Catal. A* **1996**, *137*, 105.

Scheme 1. Preparation Methods for Pd-Modified Materials

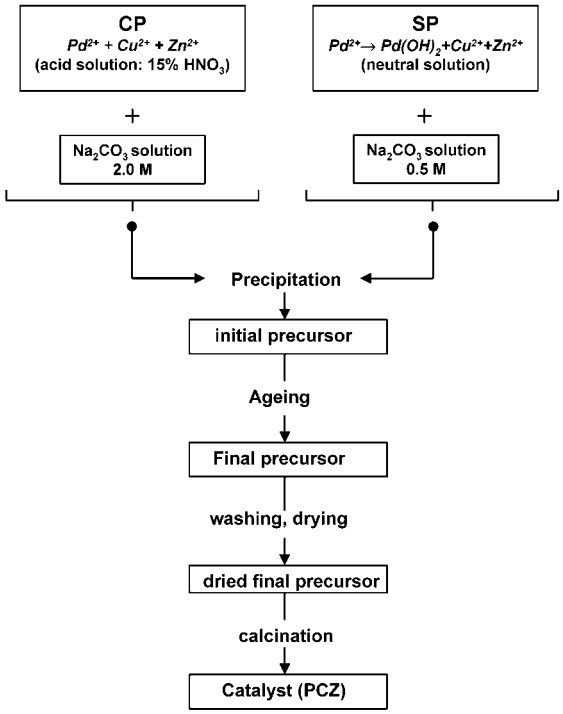

monitored in an air flow of 50 mL/min and at a heating rate of 10 K/min. Evolved gases analysis (EGA-MS) of the precursor decomposition was performed by mass spectrometry analysis. Samples of 10−20 mg were placed in a U-shaped quartz reactor incorporated in a flow system. The flow circuit was connected to a Baltzer Prisma quadrupole mass spectrometer QMS 200. A mixture of 21% O_2 in Ar was introduced at a rate of 50 mL/min, and the temperature was increased at 10 K/min while the evolved gases were continuously monitored.

Fourier transform infrared (FT-IR) spectra were recorded at room temperature on a Nicolet 510 FT-IR spectrophotometer connected to a Nicolet 680 Spectral Workstation and equipped with a DTGS detector. The sample wafers were prepared by dilution in a KBr matrix (KBr/sample = 90/10) followed by pressing at 5 tons/cm^2. The framework vibrations were obtained by placing the sample wafer directly into the infrared beam. Spectra were recorded at a resolution of 4 cm^{-1}, and 100 scans were necessary to obtain a satisfactory signal-to-noise ratio.

X-ray photoelectron spectra (XPS) were acquired with a VG Escalab 200R spectrometer equipped with a hemispherical electron analyzer and an Al Kα ($h\nu$ = 1486.6 eV) X-ray source. The samples were outgassed at room temperature within the pretreatment chamber of the spectrometer. The binding energies of Cu($2p_{3/2}$), Zn($2p_{3/2}$), Pd($3d_{5/2}$), and C(1s) core levels were determined with reference to the adventitious C(1s) signal at a binding energy (BE) of 284.9 eV. This reference gave an accuracy of ±0.1 eV. Peak intensities were estimated by calculation of the integral of each peak, after smoothing, subtraction of an S-shaped background, and fitting of the experimental curve to Lorentzian and Gaussian lines of variable proportion. Atomic ratios were then computed from the intensity ratios normalized by atomic sensitivity factors.[28]

3. Results and Discussion

3.1. Structural Characterization of the Precursors. Cu−Zn Precursor (CZ). The crystalline phase composition of the CZ precursor was determined by XRD. Peak assignments were made by inspection of the international JCPDS database. The XRD pattern of the CZ precursor is shown in Figure 1. For the sake of comparison, the powder diffraction profiles of some reference compounds (bar diagrams) are also included. The XRD pattern provides evidence for the presence of both hydrozincite and aurichalcite phases. The pioneering work of Himelfarb et al.[29] was particularly helpful to distinguish between the various Cu−Zn hydroxycarbonate phases. By means of careful XRD profile comparison, they demonstrated that aurichalcite exhibits some specific reflections at 2θ = 34.1°, 41.9°, and 50.1° (JCPDS 38-152),[30] which also appeared in the pattern of our CZ precursor. Accordingly, the crystalline nature of the CZ precursor is assigned to the presence of the aurichalcite (Au) phase.

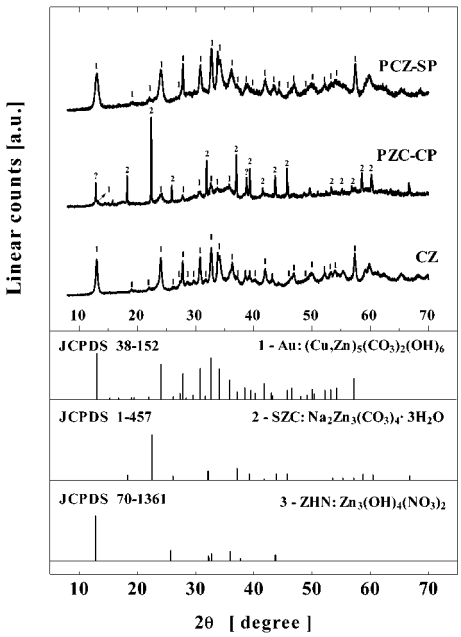

Figure 1. Powder XRD patterns of precursors, dried at 383 K. Au: aurichalcite = $(Cu,Zn)_5(CO_3)_2(OH)_6$. SZC: sodium−zinc carbonate = $Na_2Zn_3(CO_3)_4{\cdot}3H_2O$. ZHN: zinc hydroxynitrate = $Zn_3(OH)_4(NO_3)_2$.

Further evidence for the presence of aurichalcite was provided by the IR framework vibrations analysis. The IR spectrum for the CZ sample (Figure 2) coincides very well with the one published by Waller et al.[31] for aurichalcite. They stated that aurichalcite displays some characteristic fingerprint bands that are distinct from those of other hydroxycarbonate phases. In particular, the presence of specific absorption bands at 1572, 1365, 1185, and 978 cm^{-1} reveals that the aurichalcite phase is present in the precursor. The other bands at 1514, 1412, and 834 cm^{-1}, although not specific to aurichalcite because they appear in other Cu−Zn hydroxycarbonate solid solutions, were also assigned to aurichalcite. Aurichalcite, which is usually assigned the orthorhombic $B22_12$ space group,[32] has recently been shown to exist as monoclinic and twinned crystals with a $P2_1/m$

(28) Wagner, C. D.; Davis, L. E.; Zeller, M. V.; Taylor, J. A.; Raymond, R. H.; Gale, L. H. *Surf. Interface Anal.* **1981**, *3*, 211.

(29) Himelfarb, P. B.; Simmons, G. W.; Klier, K.; Herman, R. G. *J. Catal.* **1985**, *93*, 442.

(30) X-ray Powder Data File, JCPDS 38-152.

(31) Waller, D.; Stirling, D.; Stone, F. S.; Spencer, M. S. *Faraday Discuss. Chem. Soc.* **1989**, *87*, 107.

(32) Jambor, J. L.; Pouliot, G. *Can. Mineral.* **1965**, *8*, 385.

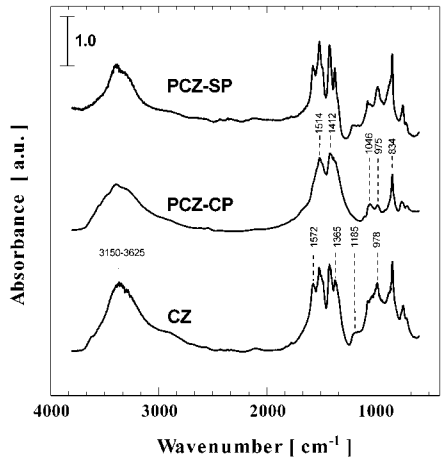

Figure 2. FT-IR spectra of precursors dried at 383 K.

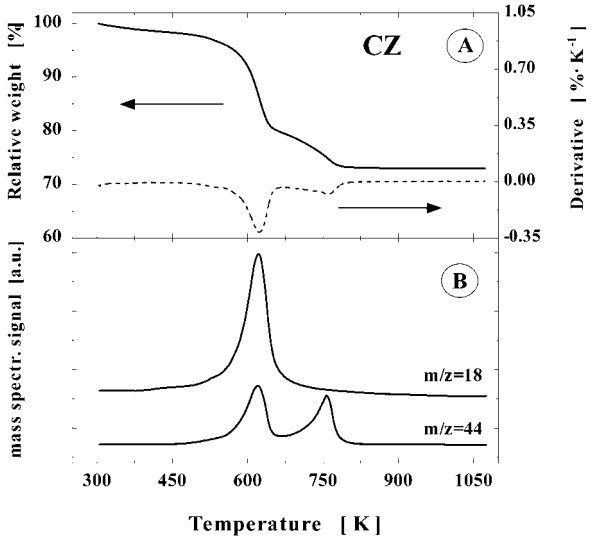

Figure 3. (A) TGA curve of the CZ precursor. The dashed line corresponds to its derivative curve. (B) MS trace for the evolution of H_2O ($m/z = 18$) and CO_2 ($m/z = 44$).

space group.[33] The structure of this system is very complex, and tetrahedral and octahedral layers alternate in the (100) direction. In contrast to the structure of hydrozincite, the former structure also contains five-coordinate metal atoms. Tetrahedral sites are probably occupied by Zn(II), while the other sites are occupied by Zn(II) and Cu(II).

Thermogravimetric and derivative curves for the decomposition of the CZ precursor in a flow of air are displayed in Figure 3A. Two clear decomposition steps can be observed: the first step relates to a 19.4 wt % weight loss with a maximum at 625 K, whereas the second weight loss is 6.7 wt % with a maximum at 760 K. To understand the mechanism of the decomposition process, evolved gases produced by thermal reactions in the solid were monitored online by mass spectrometry. The intensities of the masses $m/z = 18$ (H_2O) and $m/z = 44$ (CO_2) were simultaneously recorded over the whole temperature range covered by the decomposition process. The evolution of the decomposition products H_2O and CO_2 as a function of temperature is shown in Figure 3B. It is evident from these profiles that the first decomposition process, with a maximum at 625 K, involves the simultaneous evolution of H_2O and CO_2, whereas CO_2 is the only product resulting from further thermal decomposition. It can be seen in the mass spectrometry profile of CO_2 evolution that the area underneath each of the peaks of CO_2 is virtually the same and is approximately one-third of the H_2O decomposition peak. According to these observations, together with the preceding XRD−FT-IR analysis, and also taking into consideration literature findings,[34,35] the transformation of the CZ precursor can be described by the following consecutive processes:

$$(Cu,Zn)_5(CO_3)_2(OH)_6 \rightarrow (Cu,Zn)_5O_4(CO_3) + 3H_2O + CO_2 \quad (4)$$

$$(Cu,Zn)_5O_4(CO_3) \rightarrow (Cu,Zn)_5O_5 + CO_2 \quad (5)$$

From these profiles it is clear that temperatures as high as 800 K would be required for complete decomposition of the remaining carbonates. The overall weight loss in the TGA experiment (ca. 27.1%) is consistent with the starting monophasic material having the aurichalcite structure [i.e., $(Cu_{0.3}Zn_{0.7})_5(CO_3)_2(OH)_6$, weight loss = 26.0%].

Although not specifically relevant for the present work, an inspection of the derivative profiles shows some asymmetry, with a tail in the curves extending toward lower temperatures. This asymmetry is absent in the TGA profiles recorded at a lower heating rate (5 K/min), and so it appears that kinetic effects dominate the decomposition process.

Pd−Cu−Zn Precursor by Coprecipitation (PCZ-CP). Closer inspection of the XRD diagram (Figure 1) reveals a new phase that is ascribed to a sodium−zinc carbonate (SZC), $Na_2Zn_3(CO_3)_4 \cdot 3H_2O$ (JCPDS 1-457).[36] Fujita et al.[37] studied the evolution of precursor structures during the preparation of Cu−Zn-based catalysts, and they also detected this crystalline phase. It is important to note that no copper crystalline phases were detected in the PCZ-CP precursor apart from a very small amount of aurichalcite. This observation indicates that copper is mainly present as an amorphous compound. Remarkably, during the identification of the phases, two peaks appeared at $2\theta = 12.88°$ and 38.76°, and these were difficult to index. The appearance of such peaks had been described previously in the results presented by Fujita et al.,[37] together with the characteristic lines of SZC (JCPDS 1-457),[36] although these authors did not provide a definitive interpretation. In an attempt to reveal the identity of these two peaks, we carried out extensive research in the JCPDS database. Our search results indicated that the zinc hydroxynitrate phase (ZHN), $Zn_3(OH)_4(NO_3)_2$ (JCPDS 70-1361),[38] could be the cause of the reflection at $2\theta = 12.88°$, but the analysis of the evolved gases did not show any release of nitrogen oxides. On the basis of

(33) Harding, M. M.; Kariuki, B. M.; Cernik, R.; Cressey, G. *Acta Crystallogr. B* **1994**, *50*, 673.

(34) Stacey, M. H.; Shannon, M. *Reactivity of Solids*, Elsevier: Amsterdam, The Netherlands, 1985.

(35) Millar, G. J.; Holm, I. H.; Uwins, P. J. R.; Drennan, J. *J. Chem. Soc., Faraday Trans.* **1998**, *94* (4), 593.

(36) X-ray Powder Data File, JCPDS 1-457.

(37) Fujita, S.; Satriyo, A. M.; Shen, G. C.; Takezawa, N. *Catal. Lett.* **1995**, *34*, 85.

(38) X-ray Powder Data File, JCPDS 70-1361.

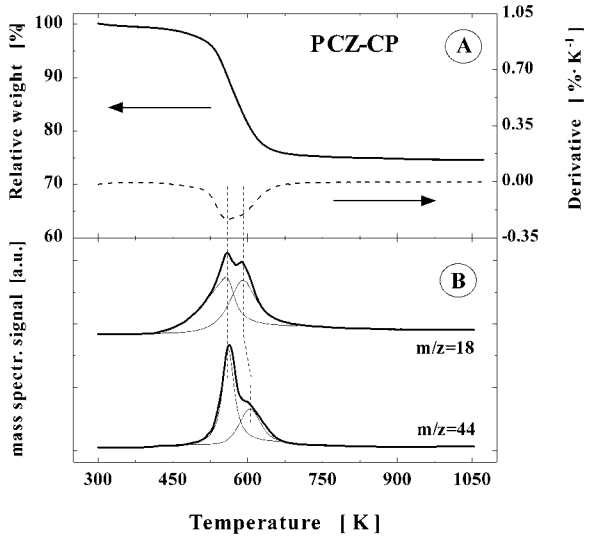

Figure 4. TGA and EGA curves for the precursor PCZ-CP.

these results, the existence of the ZHN phase was ruled out. It is proposed that these peaks might indeed belong to SZC because the information about the XRD profile of SZC in the JCPDS database (JCPDS 1-457)[36] is not very detailed.

Comparison of the TGA profiles for the CZ and PCZ-CP precursors also highlighted important differences. The decomposition curve (Figure 4A) displays two different weight losses: the first one has a maximum at 560 K, and the second is visible as a shoulder at 590 K. Both of these losses are located at lower temperatures than those in the CZ precursor. The initial loss at 560 K gave rise to the simultaneous release of carbon dioxide and water (Figure 4B) and is attributed to decomposition of $Na_2Zn_3(CO_3)_4 \cdot 3H_2O$ according to the reaction

$$Na_2Zn_3(CO_3)_4 \cdot 3H_2O \rightarrow Na_2O + 3ZnO + 3H_2O + 4CO_2 \quad (6)$$

This assignment is supported by the quantitative data derived from the EGA-MS analysis. The ratio between the amount of evolved CO_2 and H_2O was very close to the stoichiometric 4/3 value indicated by reaction 6. The second weight loss, at 590 K, also indicates a simultaneous release of water and carbon dioxide. This observation suggests that copper (because all of the zinc is taken up as the SZC phase) is present in the precursor as an amorphous copper hydroxycarbonate (Am), defined as $Cu_2(OH)_{4-2x}(CO_3)_x$. Evidence to support this hypothesis is provided by the FT-IR spectrum of the precursor (Figure 2). The absorption bands at 834, 1412, and 1514 cm^{-1}, which are characteristic of carbonate species in a malachite-like environment,[31] and the smaller bands at 1046 and 975 cm^{-1} for O−H deformations,[39] confirm that the amorphous material is a copper hydroxycarbonate. Thus, the decomposition process at higher temperature can be summarized as follows:

$$Cu_2(OH)_{4-2x}(CO_3)_x \rightarrow 2CuO + (2 - x)H_2O + xCO_2 \quad (7)$$

This single-step decomposition behavior and the temperature of its maximum at 590 K are in agreement with the results reported by Stacey and Shannon.[34] These authors carried out a detailed study on the decomposition of Cu−Zn hydroxycarbonate solid solutions and pointed out that only pure metal hydroxycarbonates (i.e., malachite and hydrozincite) decompose in one step. All of the mixed metal hydroxycarbonates decompose in two steps, as could be seen for the case of the CZ sample (eqs 4 and 5).

The stoichiometric formula of the amorphous copper hydroxycarbonate can be estimated from the EGA-MS profiles, assuming that 1 mol of H_2O produced corresponds to 2 mol of OH groups and 1 mol of CO_2 corresponds to 1 mol of CO_3^{2-}. A value for x of 0.73 was determined by following this stoichiometry. Hence, the following formula for the amorphous copper hydroxycarbonate was derived: $Cu_2(OH)_{2.54}(CO_3)_{0.73}$. Finally, assuming a nominal atomic ratio of Cu/Zn = 28.5/70 for the PCZ-CP precursor, the percentages of both phases present in the precursor are 38% Am and 62% SZC. The weight loss obtained by TGA (25.4%) was rather consistent with the stoichiometry derived from EGA-MS analysis (30.5%). The difference could be ascribed to the error inherent to the deconvolution procedure of the EGA-MS curves itself.

Pd−Cu−Zn Precursor by Sequential Precipitation (PCZ-SP). The palladium-modified precursor prepared by sequential precipitation showed an XRD pattern quite similar to that of the CZ precursor (Figure 1). However, the significantly broadened peaks of the PCZ-SP precursor indicated that the precipitate was more amorphous. This behavior may be explained by assuming that the presence of the $Pd(OH)_2$ precipitate affects the synthesis and further growth of aurichalcite. However, there is no literature evidence to support such a tempting hypothesis. Another more likely explanation, supported by literature findings in other crystalline systems,[40] could be the partial insertion of Pd(II) ions, which are formed in the $Pd(OH)_2$ solubility equilibrium, into the aurichalcite structure to form a solid solution defined as $(Pd,Cu,Zn)_5(CO_3)_2(OH)_6$. The larger size of this cation may cause a distortion of the structure.[40] The TGA−EGA profiles (Figure 5) and IR spectrum (Figure 2) are virtually identical to those of the CZ precursor.

Both Pd-modified precursors, PCZ-CP and PZC-SP, did not show evidence of any palladium compound decomposition processes. This finding indicates that the palladium hydroxide phase, which is present in the predried precipitate, is dehydrated at 393 K during the drying step and transformed into palladium oxide.

3.2. Surface Analysis of Precursors by Photoelectron Spectroscopy. The analysis of carbon, copper, zinc, and palladium electron core levels provides useful information not only about the chemical state of the elements but also about the relative proportions at the surface of the precursors. Thus, photoelectron spectra of Cu(2p), Zn(2p), Pd(3d), and C(1s) levels were recorded, and the corresponding binding energies are given in Table 1. For illustrative purposes, Figure 6 shows the Cu(2p) energy regions of the photoelectron spectra of all of the precursors. All of these spectra

(39) Shen, G. C.; Fujita, S.; Matsumoto, S.; Takezawa, N. *J. Mol. Catal. A* **1997**, *124*, 123.

(40) Basile, F.; Fornasari, G.; Gazzano, M.; Vaccari, A. *Appl. Clay Sci.* **2001**, *18*, 51.

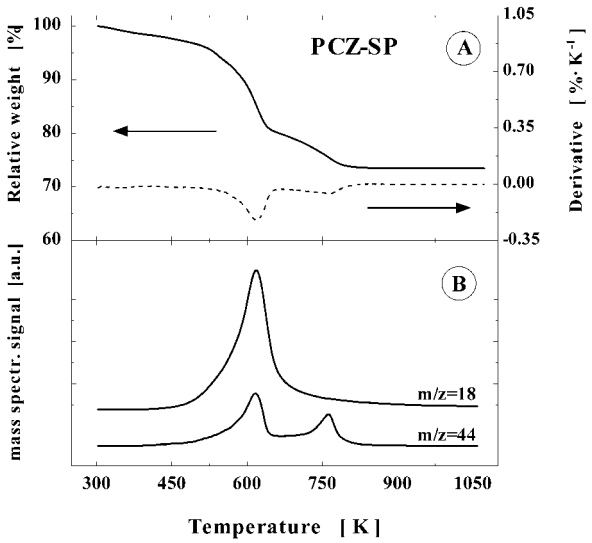

Figure 5. TGA and EGA curves for the precursor PCZ-SP.

Table 1. Binding Energies (eV) of Core Electrons for Outgassed Precursors (Room Temperature)

sample	C(1s)	Cu($2p_{3/2}$)	$\alpha_A'(Cu_{LMM})$	I_S/I_M[a]	Zn($2p_{3/2}$)	$\alpha_A'(Zn_{LMM})$
CZ	284.9 289.7	934.9	1850.9	0.61 (8.3)	1020.4	2007.8
PCZ-CP	284.9 289.7	934.6	1851.1	0.69 (7.9)	1020.2	2007.8
PCZ-SP	284.9 289.8	934.7	1851.1	0.60 (8.2)	1020.4	2007.7

[a] Values in parentheses represent the satellite splitting energies (eV).

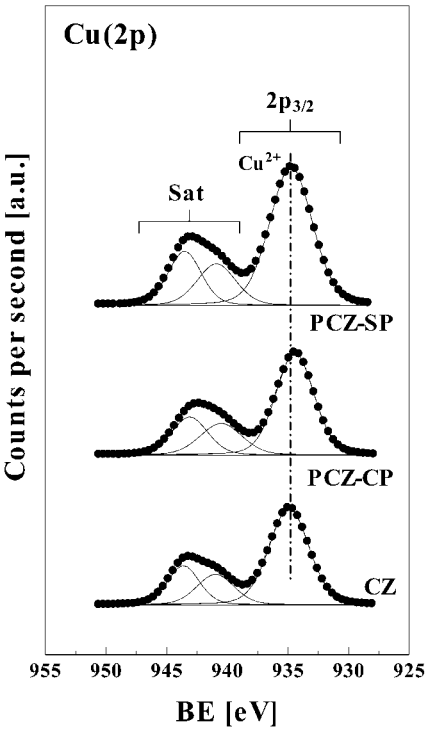

Figure 6. XPS spectra of Cu(2p) core level for precursors.

display the principal Cu($2p_{3/2}$) peak at 934.6−934.9 eV, which is characteristic of Cu(II) species.[41−44] It should be noted that the presence of Pd in the PCZ systems does not change the BE of the Cu($2p_{3/2}$) level with respect to the CZ sample. An additional way of identifying Cu(II) ions is the presence of a satellite line in addition to the principal one. The origin of this satellite is complex and has been explained in terms of shake-up processes,[45,46] final state effects,[47,48] and charge-transfer mechanisms.[49] Because the reduced copper species [Cu(I) and Cu^0] do not exhibit a satellite line, a simple way to reveal the presence of reduced copper species is to calculate the satellite-to-main line ratio (I_S/I_M). Although there are small changes within the samples, the high values of the I_S/I_M ratio (Table 1) with respect to pure CuO ($I_S/I_M = 0.5$) are within the expected values for copper(II) hydroxycarbonates.[41,50] Support for the presence of hydroxycarbonates comes from the low satellite splitting energy value observed for the samples (7.9−8.3 eV) with respect to CuO (8.6 eV).[22] These low values are in agreement with the findings of Okamoto et al.,[41] who explained them in terms of the presence of OH^- and CO_3^{2-} groups around the Cu(II) ions.

The BE for the Zn($2p_{3/2}$) level was similar (1020.2−1020.4 eV) in all of the samples. However, the full width at half-maximum (fwhm) value of nearly 3.6 eV was much higher than those for the Cu(2p) and Pd(3d) core levels. This observation indicates the presence of various environments, e.g., hydroxyl and carbonate groups, around the Zn(II) ion. The C(1s) profile exhibited two components in the spectra of all three samples (Figure 7). These spectra are characterized by a component at 284.9 eV due to adventitious carbon and a second component that occurs at a higher BE (289.7−289.8 eV), which is associated with carbonate structures.[51,52] These carbonate ions are strongly bonded to Zn(II) and/or Cu(II) ions, and their complete removal is only possible by thermal decomposition under a forced flow of air at 800 K, a situation already revealed by TGA−EGA experiments.

Finally, the Pd(3d) core-level spectra of PCZ-CP and PCZ-SP precursors are shown in Figure 8. The BE of the Pd($3d_{5/2}$) component, at 336.9 eV, of the Pd(3d) doublet is typical of palladium oxide.[22,53−55]

The aim of the Auger study was to evaluate the chemical environment of the Cu^{2+} species in the PCZ-CP sample and then to confirm the suggested presence of an amorphous copper hydroxycarbonate as EGA-MS

(41) Okamoto, Y.; Fukino, K.; Imanaka, T.; Teranishi, S. *J. Phys. Chem.* **1983**, *87*, 3740.
(42) Porta, P.; Campa, M. C.; Fierro, G.; Lo Jacono, M.; Minelli, G.; Moretti, G.; Stoppa, L. *J. Mater. Chem.* **1993**, *3*, 505.
(43) Tavares, R.; Martínez-Arias, A.; López Granados, M.; Fierro, J. L. G. *J. Catal.* **1998**, *178*, 146.
(44) Fierro, J. L. G. *Catal. Rev. Sci. Eng.* **1993**, *34*, 255.
(45) Fiermans, L.; Hoogewijs, R.; Vennik, J. *Surf. Sci.* **1975**, *47*, 1.
(46) Kim, K. S. *J. Electron Spectrosc. Relat. Phenom.* **1974**, *3*, 217.
(47) Van der Laan, G.; Westra, C.; Haas, C.; Sawatzsky, G. A. *Phys. Rev. B* **1981**, *23*, 4369.
(48) Okada, K.; Kotani, A. *J. Electron Spectrosc. Relat. Phenom.* **1997**, *86*, 19.
(49) Parmigiani, F.; Sangaletti, L. *J. Electron Spectrosc. Relat. Phenom.* **1994**, *66*, 223.
(50) Porta, P.; Fierro, G.; Lo Jacono, M.; Moretti, G. *Catal. Today* **1988**, *2*, 675.
(51) Baird, T.; Campbell, K. C.; Holliman, P. J.; Hoyle, R. W.; Stirling, D.; Williams, B. P.; Morris, M. *J. Mater. Chem.* **1997**, *7* (2), 319.
(52) Boughriet, A.; Gengembre, L.; Laureyns, J.; Recourt, P.; Langelin, H. R.; Nacer, A. *Phys. Chem. Chem. Phys.* **2000**, *2*, 1059.
(53) Iwasa, N.; Masuda, S.; Ogawa, N.; Takezawa, N. *Appl. Catal. A* **1995**, *125*, 145.
(54) Venezia, A. M.; Rossi, A.; Duca, D. G. *Appl. Catal. A* **1995**, *125*, 113.
(55) Cubeiro, M. L.; Fierro, J. L. G. *J. Catal.* **1998**, *179*, 150.

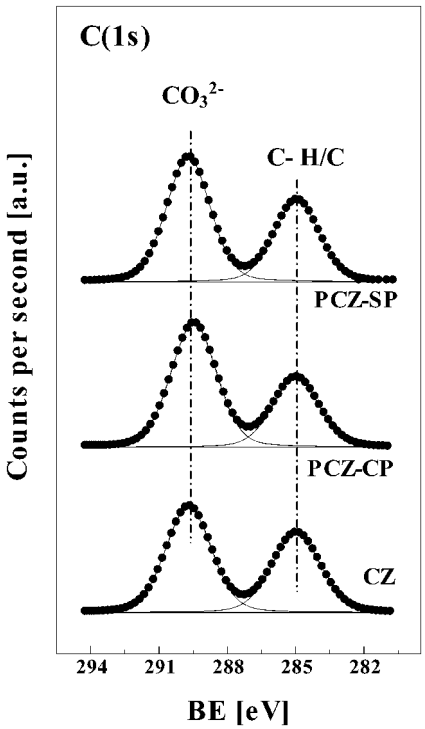

Figure 7. XPS spectra of C(1s) core level for precursors.

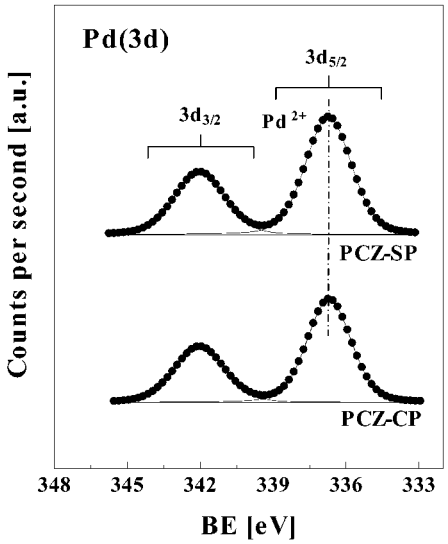

Figure 8. XPS spectra of Pd(3d) core level for precursors.

showed. The modified Auger parameters for Cu_{LMM} ($\alpha_{A'Cu}$) and Zn_{LMM} levels ($\alpha_{A'Zn}$) are defined as follows:

$$\alpha_{A'Cu} = 1486.6 + \{Cu_{LMM} - KE[Cu(2p_{3/2})]\} \quad (8)$$

$$\alpha_{A'Zn} = 1486.6 + \{Zn_{LMM} - KE[Zn(2p_{3/2})]\} \quad (9)$$

where Cu_{LMM} and Zn_{LMM} are the kinetic energies (KE) of Auger electrons for copper and zinc, respectively, and $KE[Cu(2p_{3/2})]$ and $KE[Zn(2p_{3/2})]$ are the kinetic energies of $Cu(2p_{3/2})$ and $Zn(2p_{3/2})$ core electrons. The additional value of 1486.6 eV is the energy of the incident Al Kα photons used in the X-ray source. The values of $\alpha_{A'Cu}$ and $\alpha_{A'Zn}$ for all of the samples are also given in Table 1.

The $\alpha_{A'Cu}$ values are in agreement with those reported[43,44] for copper compounds containing Cu(II) ions in their structure, indicating that Cu(I) or Cu^0 species are not present. The values for CZ and PCZ-SP, which are characteristic of Cu(II) with CO_3^{2-} groups, agree with the bulk techniques that indicated an aurichalcite structure $(Cu,Zn)_5(CO_3)_2(OH)_6$. However, a value of 1851.1 eV for $\alpha_{A'Cu}$ means that the Cu(II) species in the PCZ-CP sample are hydroxycarbonates. Therefore, the presence of an amorphous copper hydroxycarbonate in the PCZ-CP precursor, as suggested by thermal methods, is confirmed by the modified Auger parameter. Similarly, as one would expect, the $\alpha_{A'Zn}$ values fit very well with that for Zn(II) in a carbonate structure.[56]

Table 2. Surface Atomic Ratios of the Outgassed Precursors (Room Temperature)

sample	Cu/Zn[a]	Pd/Zn[a]	CO_3^{2-}/Zn
CZ	0.592 (0.44)		0.749 (0.57)[b]
PCZ-CP	0.745 (0.41)	0.045 (0.02)	1.035 (1.48)[c]
PCZ-SP	0.555 (0.41)	0.057 (0.02)	0.528 (0.56)[d]

[a] Values in parentheses represent nominal values. [b] Bulk value from a precursor aurichalcite structure defined as $(Cu_{0.30}Zn_{0.70})_5(CO_3)_2(OH)_6$. [c] Bulk value from a precursor aurichalcite structure defined as $(Cu_{0.29}Zn_{0.71})_5(CO_3)_2(OH)_6$. [d] Bulk value from a precursor composition of 38% $Cu_2(OH)_{2.54}(CO_3)_{0.73}$ and 62% $Na_2Zn_3(CO_3)_4 \cdot 3H_2O$.

The surface atomic ratios Cu/Zn, Pd/Zn, and C/Zn of the three precursors were calculated from the integral intensities of $Cu(2p_{3/2})$, $Zn(2p_{3/2})$, $Pd(3d_{5/2})$, and C(1s) peaks using the sensitivity factors given by Wagner et al.[28] These ratios are summarized in Table 2. In general, Cu/Zn ratios are higher, particularly for the PCZ-CP sample, than those corresponding to the nominal composition. Such a deviation in the CP case presumably arises from the differences in the crystal sizes of the precursor phases. On the basis of the broadening of the diffraction lines of the precursors in Figure 1, it is evident that larger crystallites of the double sodium−zinc carbonate phase are developed in the PCZ-CP sample. This fact indicates that fewer Zn atoms are exposed to the surface than in other samples, a situation that causes the Cu/Zn ratio to increase. The same reasoning applies for the Pd/Zn ratios. The surface Pd/Zn ratios observed for the two samples are 2−3 times higher than those calculated from the nominal loading. This fact suggests that small PdO particles are well dispersed on the external surface of larger crystal size SZC and Am phases. Finally, the carbonate-to-zinc [CO_3^{2-}/Zn(II)] ratios were calculated and compared with those estimated from TGA−EGA measurements (value in parentheses in Table 2).

There is a rather good agreement between the [CO_3^{2-}/Zn(II)] ratio derived from XPS and that calculated from TGA−EGA curves. However, some differences are shown. For PCZ-CP, the PdO phase may have an influence on the development of surface carbonates. The amount of surface carbonate species is much lower than that derived from TGA−EGA data, which indicates that the surface of the amorphous hydroxycarbonate and/or sodium−zinc carbonate became impoverished in carbonate. On the other hand, the amount of surface carbonates in the CZ precursor appears to be higher than stoichiometric. In this case, such a deviation (+30%) could be ascribed to residual adsorbed carbonates at the

(56) *Handbook of X-ray Photoelectron Spectroscopy, Physic Electronics*; Perkin-Elmer, Co.: Eden Prairie, MN, 1986.

Scheme 2. (A) General Scheme for the Formation of the Cu−Zn Precursors, Taken from Reference 39, (B) Proposed Mechanism for the Formation of the PCZ-CP Precursor, and (C) Mechanism for CZ and PCZ-SP Precursors[a]

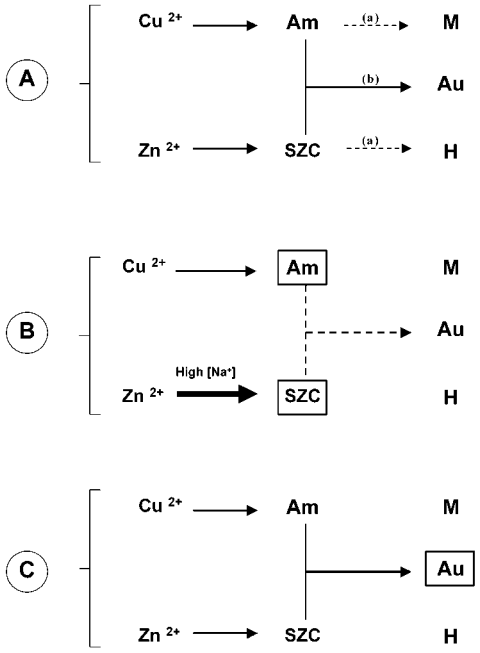

[a] Am: amorphous hydroxycarbonate. M: malachite. SCZ: sodium−zinc carbonate. H: hydrozincite. Au: aurichalcite.

surface coming from atmospheric CO_2. This is consistent with the fact that samples were outgassed at room temperature in order to keep the initial as-synthesized structure, and some adsorbed carbonates could still be present. Therefore, the [CO_3^{2-}/Zn(II)] ratio is near to the nominal one, but it comprises an extra carbonate contribution induced by the sample handling (exposure to the ambient air) and the soft pretreatment procedure.

3.3. Mechanism of Pd-Modified Precursor Formation. Data reported in this work on the bulk and surface structure of precursors were interpreted in terms of the mechanism proposed by Shen et al.[39] These authors demonstrated that the formation of the final Cu−Zn hydroxycarbonate solid solutions is achieved through the formation of certain initial compounds. They proposed the formation of an amorphous copper hydroxycarbonate and sodium−zinc carbonate as intermediate precursors prior to the formation of malachite, aurichalcite, and hydrozincite, the final compounds (Scheme 2A). Depending on the synthesis conditions, the transformation of these precursors into one or another of the final phases is favored. High carbonate concentrations in the synthesis medium [note a in Scheme 2A] favor the transformation of the amorphous copper hydroxycarbonate to malachite and sodium−zinc carbonate to hydrozincite (as in the inverse coprecipitation method: addition of the metal cations to a solution containing sodium carbonate as the precipitating agent). On the other hand, lower carbonate concentrations [note b in Scheme 2A] allow the solid-state reaction to take place between the two initial precursors to form aurichalcite (as in the coprecipitation by simultaneous addition to the reaction vessel of both metal cations and sodium carbonate: the conditions used for the preparation of our precursors).

If we accept this proposed growth precursor mechanism and take into consideration the conditions used in the preparation of our precursors, the interpretation of our results is straightforward. However, a sodium concentration effect must be considered in order to interpret our data in terms of this mechanism. Such an effect, to the best of our knowledge, has never been considered in the interpretation of the precursor structure in CuO−ZnO-based materials.

During the preparation of the PCZ-CP precursor, the metals were dissolved in HNO_3 in order to prevent hydrolysis of Pd(II). As a result, a higher concentration of Na_2CO_3 was needed to properly control the pH of the reaction medium. The presence of a high Na concentration favors the fast nucleation and crystalline growth of the sodium−zinc carbonate phase over the formation of the amorphous copper hydroxycarbonate phase (thick and thin arrows, respectively, in Scheme 2B). This kinetic imbalance in the formation of SCZ causes an unequal growth of the two phases, resulting in much bigger particles for the SZC in comparison to the Am phase. The contact area between the two intermediate phases diminishes and, as a consequence, the transformation of these two solid phases into aurichalcite is inhibited (dashed line in Scheme 2B). Traces of aurichalcite are found in the XRD profile of this precursor (PCZ-CP), indicating that the solid-phase reaction does indeed take place but that the kinetics of this reaction is very slow. In contrast, a more dilute solution of Na_2CO_3 was used during the synthesis of the precursors CZ and PCZ-SP. The lower Na concentration in the synthesis medium favors the gradual reaction between the two intermediates and leads to the formation of a well-defined crystalline aurichalcite phase (Scheme 2C).

3.4. Structural Characterization of the Calcined Precursors. All of the precursors were calcined in air at 623 K during a prolongated time (4 h). The calcination temperature was chosen on the basis of thermal sintering restrictions of CuO phase, though TGA−EGA-MS experiments indicated an incomplete decomposition at this temperature. Such a temperature is close to the higher limit allowed in order to minimize thermal sintering of copper-based catalysts. Higher temperatures, such as those required to decompose the remaining CO_3^{2-} groups, would have a large adverse effect on the catalytic activity for methanol synthesis.

Figure 9 illustrates the XRD patterns of the calcined precursors. Despite the fact that the most intense diffraction lines at $30° < 2\theta < 40°$ are overlapped, the peaks could be indexed as being due to CuO (JCPDS 80-1268)[57] and ZnO (JCPDS 36-1451)[58] phases. The lack of PdO detection by XRD in the calcined Pd-modified precursors could be ascribed to the low Pd metal loading (1.5% Pd, atomic ratio), an effect which is in agreement with the high Pd dispersion shown by XPS (see section 3.2). Comparison of the peak shapes of CuO and ZnO species shows that diffraction lines are sharper for the calcined PCZ-CP sample than for the CZ and PCZ-SP counterparts, a consequence of the larger dimensions of the CuO and ZnO crystalline particles. The mean crystalline sizes (D) of CuO and ZnO were determined from the line broadening of the (111) ($2\theta = 38.77°$) and

(57) X-ray Powder Data File, JCPDS 80-1268.
(58) X-ray Powder Data File, JCPDS 36-1451.

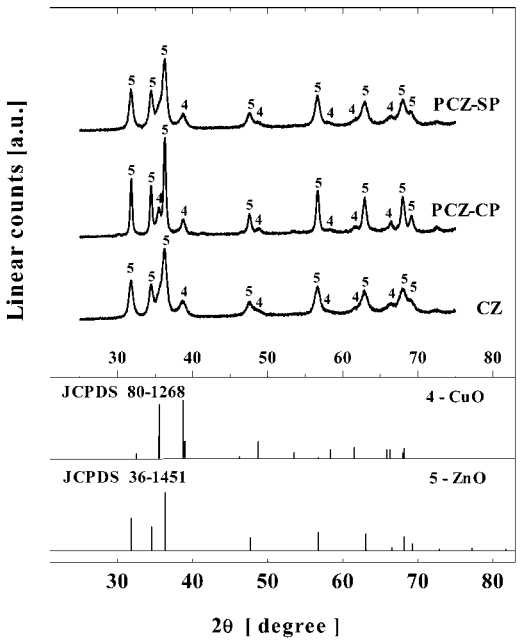

Figure 9. Powder XRD patterns for the calcined (623 K) precursors.

Table 3. Effect of the Precursor Structure on the CuO−ZnO Particle Sizes Present in the Final Calcined Precursor

	precursor[a]		*D*, crystal size (nm)	
sample	XRD	TGA−EGA	CuO	ZnO
CZ	Au	Au	9.3	13.0
PCZ-CP	SZC	SZC-Am	15.7	26.2
PCZ-SP	Au	Au	9.6	14.3

[a] Phases detected by XRD and TGA−EGA experiments. Au: aurichalcite = $(Cu,Zn)_5(CO_3)_2(OH)_6$. Am: amorphous copper hydroxycarbonate = $Cu_2(OH)_{2.54}(CO_3)_{0.73}$. SZC: sodium zinc carbonate = $Na_2Zn_3(CO_3)_4{\cdot}3H_2O$.

(100) ($2\theta = 31.77°$) diffraction lines, respectively, using the Scherrer equation after Warren correction for instrumental line broadening, $D = K\lambda/\beta \cos\theta$ with $K = 0.9$. Owing to the overlap of the CuO(111) and CuO(200) reflections in the range $37° < 2\theta < 41°$, it was also necessary to decompose the XRD profile into two contributions by applying curve-fitting procedures. It must be noted that the Scherrer formula should not be used for absolute determinations because of its failure to account for the particle size distribution and the uncertainty in correcting for instrumental line broadening. For this reason, X-ray line broadening calculations are used to obtain a relative measure of the average crystalline size.

The crystalline sizes of CuO and ZnO estimated for the calcined samples are listed in Table 3. The precursor structures obtained from XRD and TGA−EGA analysis are also included for the sake of comparison. The CuO crystal sizes of the CZ and PCZ-SP samples are virtually the same, at approximately 9 nm, while that of PCZ-CP is nearly 16 nm. The same trend is observed for the ZnO phase, although the particle size is larger than that for CuO. If we consider the precursor phases as summarized in Table 3, the mixed oxide materials prepared from the decomposition of aurichalcite (CZ and PCZ-SP) show smaller CuO particle sizes, while PCZ-CP prepared from independent copper and zinc precursor phases (i.e., sodium−zinc carbonate and amorphous copper hydroxycarbonate) has larger particles. The presence of independent Cu and Zn phases in the PCZ-CP precursor inhibits the interaction between CuO and ZnO in the calcined state, resulting in an increase in the particle size of both oxidic phases. However, the decomposition of mixed Cu−Zn hydroxycarbonate precursors such as aurichalcite, in which Cu and Zn are atomically dispersed in a hydroxycarbonate matrix, provides a high interdispersion of CuO and ZnO phases during calcination. This results in a smaller crystal size than those obtained when the oxides are derived from independent copper and zinc precursor phases, as in the case of CP.

The major relevance of these results is derived from the fact that Pd-containing materials have been used as modified catalysts for the methanol synthesis reaction. An optimal method to introduce palladium into CuO−ZnO methanol synthesis catalysts should not decrease the copper phase dispersion. Copper is required to be highly dispersed because the active sites involved in the synthesis of methanol require surface copper. The sequential precipitation method maintains the CuO dispersion at about the same value as that for the palladium-free CZ sample, whereas the coprecipitation procedure results in a poorer dispersion of copper. This information reveals the importance of the method of incorporation of palladium, and it is clear that apparently minor details, such as the precipitation order, have a remarkable influence on the properties of the active CuO phase.

Finally, the precursor structure of the Pd-modified materials characterized here could have important implications for catalytic applications in the hydrogenation of CO_2 to methanol. Specifically, the modified PCZ-SP calcined sample could be of interest because Pd is believed to enhance the methanol yield by means of hydrogen spillover. A study into this hypothesis will be reported in a later paper.[59]

4. Conclusions

The results presented in this study show that the surface and bulk structures of Pd-modified precursors depend on the palladium incorporation methodology. Such an effect is not caused by the palladium incorporation itself but comes from the preparation conditions used during synthesis, specifically sodium concentrations. The genesis and growth of the precursors is explained by means of Shen's initial-stage precursor mechanism[39] and the effect of sodium concentration as a kinetic factor in that precursor formation mechanism. The higher Na concentration used for the coprecipitated palladium material (PCZ-CP) influences the growth of the initial-stage precursor and gives rise to the formation of independent Cu and Zn phases in the final precursor. This fact inhibits the further interaction between CuO and ZnO during the calcination step and results in an increase in the particle size of both oxidic phases. The lower sodium concentration used during the synthesis of CZ and PCZ-SP precursors favors the development of a aurichalcite phase in both materials. Aurichalcite, a crystalline phase in which Cu and Zn

(59) Melián-Cabrera, I.; López Granados, M.; Fierro, J. L. G., submitted for publication.

are atomically dispersed within the structure, leads to highly interdispersed copper and zinc oxides with crystal sizes that are smaller than those when the oxides are derived from independent copper and zinc precursor phases.

Acknowledgment. This work was supported by CICYT (Spain) under Grant QUI98-0877. I.M.-C. thanks the Ministry of Education and Science for a fellowship.

CM011281S